

Ceramic Membranes: Materials – Components – Potential Applications

Wilhelm A. Meulenber^{[1,2],*}, Falk Schulze-Küppers^[1], Wendelin Deibert^[1], Tim Van Gestel^[1], Stefan Baumann^[1]

Abstract

Gas separation in dense ceramic membranes is driven by the partial pressure gradient across the membrane. The mixed conducting materials most commonly used are single-phase perovskites or fluorites. In recent years, the development of dual-phase systems combining a mixed ion-conducting and electron-conducting phase has increased. The advantage is that a larger number of very stable materials systems is available. The membrane designs currently used include planar, tubular, hollow-fiber, and honeycomb membranes. Each of these designs has specific advantages and disadvantages, depending on the application. Innovative joining concepts

are also often needed due to the high temperatures involved. These usually involve the use of glass-ceramic sealants or reactive metal brazes. Applications focus either on the separation of gases alone, i.e., the supply of oxygen or hydrogen, or on membrane reactors. In membrane reactors, a chemical reaction occurs on one or both sides of the membrane in addition to gas separation. The supply of gases is of potential interest for power plants, for the cement, steel, and glass industries, for the medical sector, and for mobile applications. Membrane reactors can be used to produce base chemicals or synthetic fuels.

Keywords: Ceramics, Membranes, Membrane reactors, Solid electrolytes

Received: October 02, 2019; *accepted:* October 08, 2019

DOI: 10.1002/cben.201900022[‡]

1 Introduction

Ceramic membranes are used to separate gases from gas mixtures or to produce chemicals (e.g., syngas, base chemicals, or synthetic energy carriers) in situ within membrane reactors [1]. These membrane reactors are modular and can theoretically be utilized wherever unexploited heat or power is readily available, making them highly efficient and flexible.

Since the availability of renewable energy is currently soaring, there is urgent demand for flexible energy storage options and methods for synthesizing chemical energy carriers. These energy carriers can be produced by means of ceramic gas separation membranes in the form of membrane reactors and can subsequently be converted back into energy using existing infrastructure. They can therefore be used to reliably bridge periods when very little energy from renewable sources is fed into the grid, thus avoiding the resulting high electricity prices. The broad range of membrane reactor processes that exist means that the ambient conditions present in the different processes vary considerably. Membranes and components can be tailored to many of these processes by adapting the material properties and microstructures. Tailoring membrane and reactor designs to a specific process, and subsequently integrating them into the overall process in a targeted manner, facilitates

high efficiencies and prevents membrane modules from being exposed to unnecessary loads.

There are two different types of ceramic gas separation membranes: microporous membranes and dense membranes. In porous membranes, the process of material separation is based on the principles of size exclusion and/or adsorption and desorption effects. Ceramic membranes are more expensive to


^[1] Prof. Wilhelm A. Meulenber (corresponding author), Dr. Falk Schulze-Küppers, Dr. Wendelin Deibert, Dr. Tim Van Gestel, Dr. Stefan Baumann

Forschungszentrum Jülich GmbH, Institute of Energy and Climate Research – Materials Synthesis and Processing (IEK-1), 52425 Jülich, Germany.

E-Mail: w.a.meulenber@fz-juelich.de

^[2] Prof. Wilhelm A. Meulenber
University of Twente, Faculty of Science and Technology, Inorganic Membranes, P.O. Box 217, 7500 AE Enschede, The Netherlands

[‡]Updated version of DOI: <https://doi.org/10.1002/cite.201900019>

 This is an open access article under the terms of the Creative Commons Attribution License, which permits use, distribution and reproduction in any medium, provided the original work is properly cited.

produce than polymer membranes and are therefore used in applications where polymer membranes cannot be utilized due to lower separation performances, higher temperatures, or aggressive ambient conditions. Fig. 1 shows examples of separation applications on the basis of membrane pore size. Potential applications of microporous membranes include the purification and treatment of water and chemicals, the dehydration of alcohol, a range of medical applications, and separation tasks in the food industry.

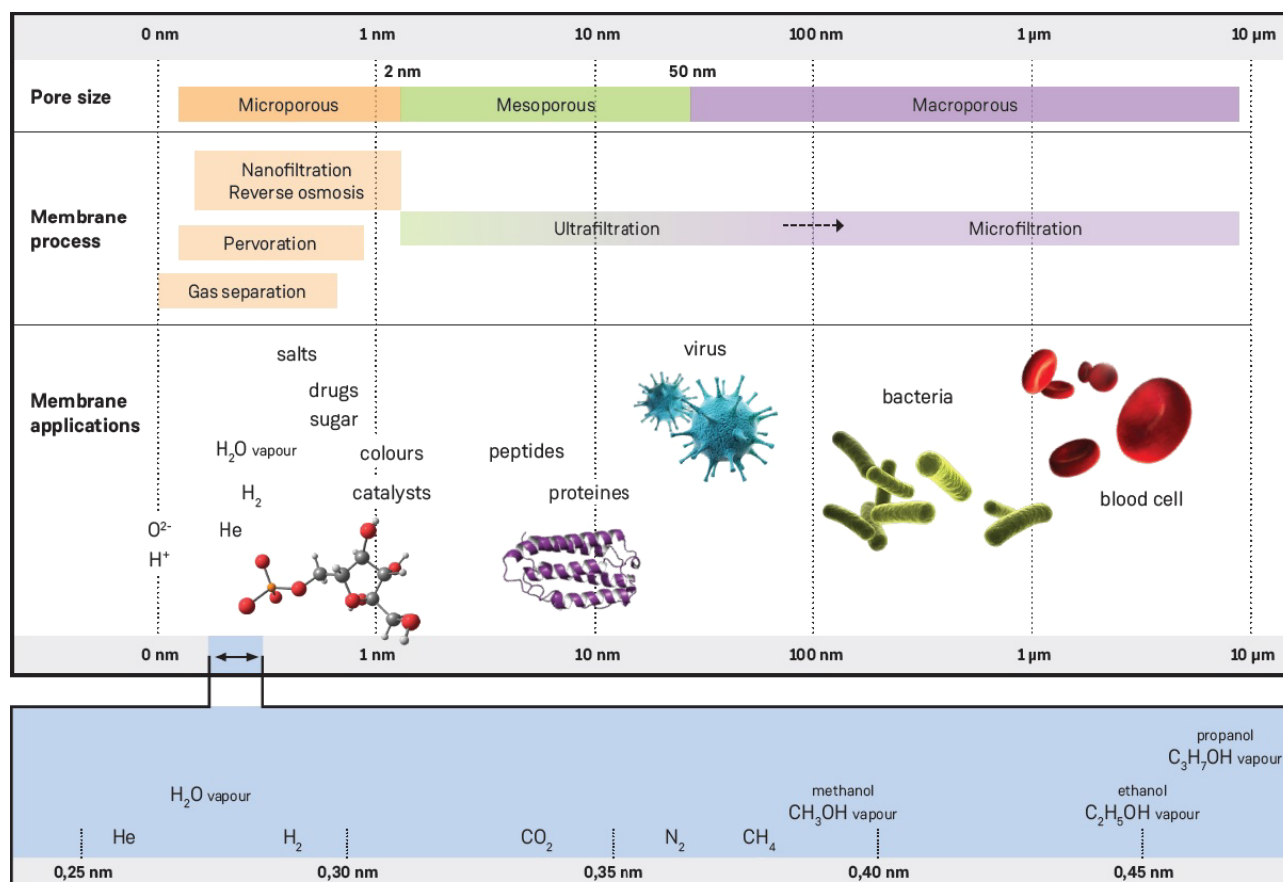
While ceramic membranes with pore sizes above 1 nm are commercially available and already utilized in a variety of sectors, gas separation membranes with a pore size of ca. 0.5 nm and lower are still in the research and development stage.

In contrast to microporous membranes, material separation in dense ion-conducting ceramic membranes is based on diffusion processes. These involve the movement of ions through the crystal lattice. Electron transport may also take place in the lattice. The diffusion process is thermally activated, requiring operating temperatures of several hundred degrees Celsius. Since there is almost no limit to the selectivity of the separation mechanism, these membranes are equally suited to producing high-purity gases and chemicals in reactors. To date, these dense membranes have been studied and utilized in applications producing pure oxygen or hydrogen in fuel cells, electrolyzers, membrane reactors, and solid-state electrolyte batteries.

In order to achieve the required performance, the membranes are fabricated as a thin layer (<100 µm) on a porous substrate. Apart from performance, other important criteria for future applications include long-term stability under corrosive conditions and mechanical loads as well as the technology used to join the membrane and the housing. The way in which membranes are integrated into a system and operating conditions are adjusted, holds great potential for the efficient and sustainable use of membranes. In addition, tailor-made materials can also be developed for long-term use. Depending on the process, these materials must exhibit chemical stability in oxidizing or strongly reducing conditions, and often also in atmospheres containing $\text{H}_2\text{S}/\text{SO}_x$, CO_x , or NO_x .

2 Dense Membranes

In principle, dense membranes are gas-tight; mass transport occurs via ion diffusion through the crystal lattice. The membranes are also electrically conducting, which enables charge compensation. These mixed ionic-electronic conductors (MIECs) can transport either oxygen ions or protons and can therefore be used to separate pure oxygen from the ambient air or to purify hydrogen in chemical processes.



Pictures (from left to right): @ollawella - stock.adobe.com • @petarg - stock.adobe.com • @simone_n - stock.adobe.com • @norman blue - stock.adobe.com • @psdesign1 - stock.adobe.com

Figure 1. Applications of ceramic membranes based on pore size.

2.1 Materials

When it comes to selecting materials, two basic options are available: single-phase ceramics and composites. Since transport (see Sect. 2.2) in single-phase MIECs is effected through defects (vacancies) in the crystal lattice, there is a trade-off between permeability (as many mobile defects as possible) and stability (as few mobile defects as possible). In composite materials, two separate phases can be chosen with ionic and electronic conductivity, respectively, which are stable under application conditions. However, these phases must be compatible both chemically and in terms of their thermal expansion behavior. In addition, the proportion of the ion-conducting phase should be maximized to keep the effective area for ion transport as large as possible, while making sure that the electron-conducting phase percolates in the matrix, thus ensuring charge compensation.

High-MIEC ceramics are frequently found in the perovskite system $\text{ABO}_{3-\delta}$, where A is one or several elements of the lanthanide series (La, Pr, Nd, etc.) or alkaline earths (Ba, Sr), and B is a transition metal (Mn, Cr, Ti, Co, Fe, Ni) [2]. Ferrites and cobaltites in particular offer high permeability (in combination with low stability). Strontium-titanate-based materials are a promising alternative [3, 4] with much higher stability. In composites, doped ZrO_2 or CeO_2 are most commonly used as ion conductors. These are sintered with electron-conducting ceramics to form a composite material [5].

In the field of proton-conducting membranes for gas separation, fluoritic materials such as $\text{La}_{6-x}\text{WO}_{12-\delta}$ (LWO) are promising candidates due to their chemical stability and comparatively high permeability to hydrogen [6–13]. Other suitable material classes include niobates (e.g., LaNbO_4) and pyrochlores (e.g., $\text{La}_2\text{Zr}_2\text{O}_7$) [14, 15]. If an external electric circuit is used, perovskite electrolytes are an attractive option. The BaZrO_3 - BaCeO_3 system is the most relevant here, since the combination of the two oxides offers a good trade-off between stability (primarily in atmospheres containing CO_2) and high proton conductivity. Y_2O_3 is also added to increase the concentration of vacancies [16–22]. In composite materials, it is possible to combine materials that conduct only protons with others exhibiting high electronic conductivity. As a consequence, the most frequently used combinations are those of the BaZrO_3 - BaCeO_3 system mentioned above (perovskite, proton conductor) with Gd-doped CeO_2 (CGO, fluorite, electron conductor) [23].

2.2 Transport Through Dense Membranes

In oxygen transport membranes (OTMs), diffusion occurs when an oxygen ion “hops” to a neighboring vacancy. These movements are distributed statistically unless a driving force is present. When a chemical potential gradient (O_2 partial pressure) is applied, ion hopping occurs preferably from the high-pressure side to the low-pressure side of the membrane, resulting in effective oxygen ion diffusion. On the side where the oxygen partial pressure is high, the vacancies become occupied by oxygen ions produced on the oxide surface by ionization and dissociation from molecular oxygen absorbed from the gas

phase. On the side where the partial pressure is low, the oxygen is released again into the gas phase. In the steady state, the oxygen diffusion j_{O_2} is described by the Wagner equation [24]:

$$j_{\text{O}_2} = \frac{RT}{16F^2} \sigma_{\text{amb}} \frac{1}{L} \ln \frac{p'_{\text{O}_2}}{p''_{\text{O}_2}} \quad (1)$$

where R is the gas constant, T the temperature, F the Faraday constant, σ_{amb} the ambipolar conductivity, L the membrane thickness, and p'_{O_2} and p''_{O_2} the oxygen partial pressure on the sides that are high and low in oxygen, respectively.

$$\sigma_{\text{amb}} = \frac{\sigma_{\text{ionic}} \sigma_{\text{electronic}}}{\sigma_{\text{ionic}} + \sigma_{\text{electronic}}} \quad (2)$$

Proton-conducting oxides usually contain no H^+ ions in their ground state. These ions must be taken up from the environment and subsequently transported through the crystal lattice of the membrane material. The uptake of H^+ may occur via the following two reactions [25]:



where $\text{O}_{\text{O}}^{\times}$ is the oxygen on the regular lattice site, $\text{OH}_{\text{O}}^{\bullet}$ the hydroxide defect on the oxygen lattice site, e' the electron, and $v_{\text{O}}^{\bullet\bullet}$ the oxygen vacancy.

The protons that have been taken up can move through the crystal lattice of hydrogen transport membranes (HTMs) via two different transport mechanisms. The first, referred to as the “vehicle mechanism”, transports protons by means of diffusion of the entire hydroxide defect via the vacancy mechanism, in the same way as oxygen ion diffusion [26]. The second, known as the “Grotthius mechanism”, involves protons in the crystal lattice “hopping” from one oxygen ion to the next [25].

The total flux of hydrogen through a ceramic membrane is contingent on the proton concentration, the mobility, and the driving force (H_2 partial pressure gradient). These correlations are illustrated in Wagner’s transport theory for hydrogen separation membranes [27]:

$$j_{\text{H}^+} = \frac{-RT}{2F^2L} \int_1^{\Pi} \sigma_e \cdot t_{\text{H}^+} d \ln p_{\text{H}_2} \quad (5)$$

The equation includes process parameters (T : temperature, p_{H_2} : hydrogen partial pressure), material parameters (σ_e : electronic conductivity, t_{H^+} : transport number for protons), a geometry parameter (L : membrane thickness), the gas constant R , and the Faraday constant F .

2.3 Microstructure of Dense Membranes

Since the permeation rate of a membrane – irrespective of the transport mechanism involved – is inversely proportional to its thickness, membranes should always be fabricated as a thin layer on a porous substrate [28] (Fig. 2).

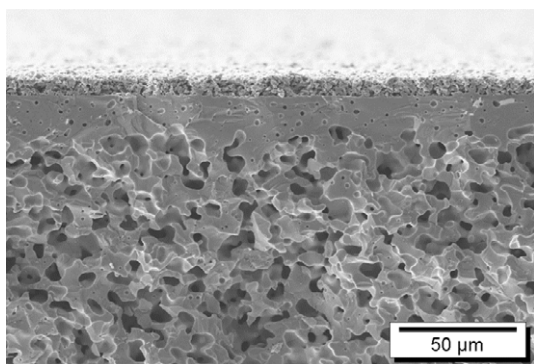


Figure 2. Fracture surface of a thin dense oxygen transport membrane on a porous substrate with surface activation on the upper surface.

The thickness is typically in the range of a few 10 μm [29–33]. Thicknesses of less than 10 μm have already been achieved, but this results in only a minor performance increase [34] and leaks become far more likely. The reason for the low increase in performance is the porous substrate, since in the case of very high permeation rates, gas diffusion through the pore network is a limiting factor [35, 36].

In order to improve gas transport through the porous substrate, the microstructure must be adapted, i.e., the number, size, and length of the transport paths. A greater number of transport paths with the same pore sizes can be achieved by increasing pore content (porosity). However, this usually has an adverse effect on mechanical stability. The porosity that is tolerable for mechanical stability depends on the mechanical properties of the substrate material [37–40]. Transport paths can be enlarged by increasing the pore opening diameters, making gas diffusion instead of Knudsen diffusion the dominant transport mechanism. This requires pore opening diameters of more than 20 μm [36]. The length of the transport paths can be described in terms of tortuosity, i.e., the ratio of path length to substrate thickness. The minimum tortuosity is 1, where the path length corresponds to the substrate thickness. Tortuosity usually decreases with increasing porosity. Different manufacturing technologies can be used to vary the shape and tortuosity of the pore channels. For example, freeze casting and phase-inversion casting produce straight channels with defined diameters.

In cases where the performance limitation can be overcome by optimizing the substrate microstructure, it will, however, converge towards a limiting value. The reactions of ion insertion and extraction on the membrane surface become increasingly rate-determining, because they occur at a progressively slower pace than ion transport through the membrane or gas transport through the substrate, respectively. In order to accelerate the insertion and extraction reactions, the reactivity of the surfaces can be improved using catalysts, or the surface area can be increased geometrically by means of a porous layer. The aim is to make the active area as large as possible while keeping layers thin in order to avoid limitations caused by gas diffusion processes [41–43].

2.4 Fabrication of Dense Membranes

The entire process of permeation must be studied in detail to identify the ideal membrane architecture and the appropriate manufacturing techniques. In addition to these aspects, which are related to the microstructure, the design of the membrane module determines external mechanical loads, which in turn have an impact on the required microstructure and thus the manufacturing techniques.

The different approaches to membrane modules are based on different membrane geometries, i.e., tubular, planar, hollow-fiber, and honeycomb structures. It has been shown that each of these designs has specific advantages and disadvantages, so that each individual case needs to be evaluated separately with a view to application requirements and available technology [44].

Planar membrane structures can be produced by means of multi-axial pressing, extrusion, or tape casting. Development currently focuses on tape casting because pressing has considerable drawbacks for mass production, and extrusion only allows for components with limited lateral dimensions. Tape casting, in contrast, offers a high degree of flexibility in terms of the size and design of flat ceramic components as well as in mass production, as is shown by the production of ceramic components in the field of electronics [45]. Pore-forming agents such as graphite or starch can be added to the slips to introduce the desired porosity [46]. The green tapes can be produced in a simple and reliable manner. In addition, multi-layer components can be fabricated through the laminating or sequential tape casting [28, 46] of different layers, followed by a co-sintering step.

Sequential tape casting was developed to reduce the number of foils to be laminated [46]. In this method, the first step consists of casting the thin membrane layer. After drying, a similar slip with a defined amount of pore-forming agents is cast onto the first layer. Because the same solvent is used, some of the additives contained in the membrane layer will dissolve again, joining the foils together. In the case of planar modules, a particular challenge is posed by the manifold different gas streams, i.e., supply, retentate, sweep, and permeate. The planar membrane components can be integrated into a module using metal or glass sealants or seals between the membrane layer and the metal housing [47, 48]. Analogous to planar solid oxide fuel cells, membrane components can be inserted into stackable metal frames to achieve high packing densities [49, 50].

Most membranes are tubular in shape. They can be fabricated in any size down to hollow fibers and combined to form membrane bundles. Tubular membranes are usually produced by extrusion. One of the greatest challenges in fabricating tubular membrane modules is the gas-tight connection of each individual tube to the metal housing. This is frequently addressed by cooling the metal base plate of the module to temperatures below 200 $^{\circ}\text{C}$, which facilitates the use of simple sealing techniques such as crimping or bonding. However, these processes involve a significant loss of active membrane area because a sufficient flux of oxygen through the membrane can only be achieved at temperatures starting from 600–700 $^{\circ}\text{C}$.

Reducing the membrane diameter to increase the ratio of surface area to volume led to the development of ceramic capil-

laries, which are often referred to as hollow fibers. These are either extruded to a given minimal diameter or spun using the phase-inversion method developed for polymer fibers [51]. If the inner diameters are small, the capillaries produce a major pressure drop along the longitudinal axis. This means that, depending on the application requirements, the length of the capillaries must be limited. As a consequence, a large number of capillaries must be used per module, and each of them must be sealed individually. This still constitutes a considerable challenge.

Schulz et al. [52] bundled seven capillaries in a tube made of the same material using an all-ceramic high-temperature seal. This strategy reduces the number of critical joints between ceramic and metal materials and minimizes the use of additional sealants, such as glass. Multi-channel tubes and honeycomb structures have also been developed and fabricated by means of extrusion. However, the reliable production and reproducibility of the connections for the homogeneous distribution of the gases between the different channels poses another significant challenge here.

2.5 Current Research Topics

Due to the multitude of potential applications and ambient conditions, there is great demand for materials that are adapted to specific requirements. Doping allows existing high-flux materials to be stabilized [53–58] and the performance of chemically very stable materials to be improved [3, 59–63]. However, materials development is currently focused on composites, both because a large variety of material combinations is available and because their microstructure can be tailored to control the performance and stability of the membrane.

To further improve the performance of membranes, novel microstructures that allow gas to be transported more efficiently through the substrate are being studied based on transport models. Transport modelling allows bottlenecks in the membrane structure to be identified at an early stage. This means that the modelling results can be factored into the choice of existing production technologies and can help to substantiate the need for new production technologies. For example, freeze casting [36, 64] and phase-inversion tape casting [65–67] are currently being investigated and used for the production of particularly straight channel structures and defined pore opening diameters. These two methods are suitable for producing both planar and tubular modules, including capillaries.

Due to the sheer number of membrane applications, the need for membrane prototypes with tailored microstructures and materials has never been greater. Prototype production requires methods that are flexible in terms of both the shapes that can be created and the materials used. Additive and subtractive manufacturing methods are therefore ideal for this purpose. Complementary to materials and microstructure development, methods such as binder jetting and photo-polymerization are currently being advanced to shorten iteration cycles in research and development [68].

Despite the fact that membrane modules for the supply of pure oxygen and hydrogen have already been developed on a

pilot scale within various EU programs (HETMOC [69], GREEN-CC [70–72], and ELECTRA [73]), and that industrial-scale plants have now been established by the US companies Praxair and Air Products [74], there is still a pressing need for further development. In addition to module design and structure, another challenge yet to be fully met is the high-temperature joining of thin supported membranes to assemble a reactor. Current research is concerned with issues relating to the chemical compatibility between the membrane material and the metal, to heat expansion behavior, and to the mechanical stability at the joint.

3 Porous Membranes

Porous ceramic membranes consist of a robust porous substrate onto which one or several porous ceramic layers are applied. These membranes are currently used worldwide in microfiltration (MF) for separating colloidal particles or dissolved materials from a solvent (water, organic solvent) [75–76]. However, particularly fine-pored microporous membranes are now increasingly considered as potential candidates, e.g., for nanofiltration (NF), gas separation (GS), and the separation of liquids (pervaporation, vapor separation) (see Fig. 1). These microporous membranes consist of a combination of macroporous, mesoporous, and microporous layers. The first two are intermediate layers, whereas the topmost microporous layer with the finest pores is able to selectively let liquid water, water vapor, or smaller gas molecules such as He, H₂, or CO₂ pass through. The pore size d_p of the membrane coating is usually classified according to the IUPAC definition: macroporous ($d_p > 50$ nm), mesoporous (2 nm $< d_p < 50$ nm), and microporous ($d_p < 2$ nm).

3.1 Materials, Microstructure

In practice, a microporous membrane device has a macroporous substrate, at least one mesoporous intermediate layer, and at least one microporous top layer, all arranged on top of each other in that order. An example of such a structure is shown in Fig. 3.

The substrate materials are often tubular porous structures produced by means of extrusion and designed as single-channel or multi-channel elements. Different materials can be utilized for this purpose, but α -Al₂O₃ is most frequently used. TiO₂, ZrO₂, SiC, and combinations of these materials are also regularly employed. Furthermore, membranes with a porous metal substrate have also been investigated [77]. In order to maximize the flux through the membrane device, the substrate generally has a graded structure with multiple layers. The average pore size of the actual substrate structure is usually in the range of >1 – 20 μ m. Suspension methods are used to coat the substrate with several macroporous layers with successively smaller pore sizes, so that the final pore size is in the range of approximately 50–200 nm. It should be mentioned here that apart from tubular geometries, other structures are also available, such as planar and honeycomb designs. In addition, simple single-layer ceramic discs with pore sizes of approximately

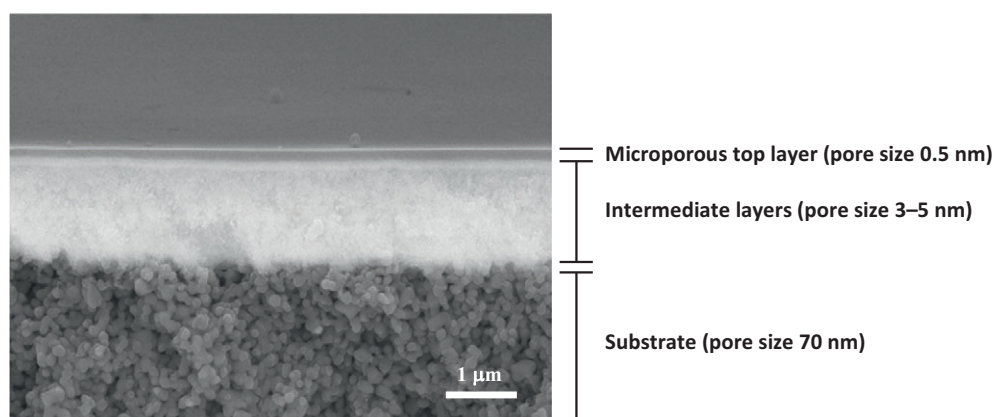


Figure 3. Fracture surface of a multi-layer microporous membrane device.

50–100 nm are often used for research purposes, where the substrate's transport resistance plays only a minor role.

For the mesoporous membrane coatings, the same materials are usually employed, with Al_2O_3 in the form of $\gamma\text{-Al}_2\text{O}_3$. The latter has been very popular in the membrane community for a long time because it can be relatively easily deposited as a thin film with the desired properties (homogeneous surface, small pores with a diameter of ~ 3 nm, narrow pore size distribution). $\gamma\text{-Al}_2\text{O}_3$ -based membranes are not suitable for many real-life applications, however, because the material has insufficient chemical and hydrothermal stability. The other membranes currently on the market (e.g., TiO_2 , ZrO_2) offer much higher chemical stability, but they are not resistant to high temperatures and water vapor (hydrothermal conditions) and are therefore of limited use in applications such as gas or vapor separation. The focus of our work for a number of years has been on thermally stabilized materials. Specific examples include stabilized ZrO_2 (8% Y_2O_3) and CeO_2 (10% Gd_2O_3) membranes with pore sizes ranging from 3 to 5 nm [78]. We found that these are able to withstand temperatures of up to 750°C and hydrothermal conditions (15 bar, 300°C) without damage. In addition, their chemical stability has been observed at a pH of 14.

In order to achieve a separation effect in the processes described above, the mesoporous membrane layers are further modified by adding one or more microporous layers. The resulting graded membrane is usually referred to as a microporous membrane. The microporous top layers can be either crystalline or amorphous. The most frequently used materials include: (a) amorphous SiO_2 and metal-doped SiO_2 [79–80], (b) hybrid SiO_2 (contains carbon atoms in addition to SiO_2) [81–82], (c) oxide ceramics free from SiO_2 (e.g., $\text{TiO}_2/\text{ZrO}_2$) [83–84], (d) non-oxide ceramics (e.g., carbon, silicon carbide) [85–86], and (e) crystalline zeolites [87–88].

SiO_2 -based membranes were first developed several decades ago. They usually have a microporous SiO_2 top layer with a pore size ≤ 0.5 nm deposited on a substrate coated with mesoporous $\gamma\text{-Al}_2\text{O}_3$. These membranes have attracted considerable interest ever since they emerged because their separation properties are suitable both for vapor separation and gas separation. In practice, however, their use is limited to dry applications because the material is very sensitive to water. Hybrid SiO_2 membranes containing carbon (HybSi©), which have been on

the market for about 10 years, are more stable in water, but have so far only been deposited onto mesoporous $\gamma\text{-Al}_2\text{O}_3$ substrates, resulting in an unsatisfactory overall stability of the entire membrane device. Such membranes are also less suitable for the separation of the smallest gas molecules (He , H_2) from larger ones (e.g., CO_2 , N_2 , CH_4) using a molecular sieving process because the pore diameter exceeds 0.5 nm. Zeolite membranes are particularly well suited for pervaporation and vapor separation applications, since at approximately 0.4 to 0.5 nm, their pore size distribution is extremely narrow. However, the disadvantage of the zeolite A membrane currently on the market lies in its limited resistance to acids and alkaline solutions. In addition, the gas separation performance of zeolite membranes is usually not very high, a fact often ascribed to the high concentration of mesoporous defects throughout the material.

In recent years, graphene, a two-dimensional single layer of carbon atoms consisting of sp^2 -hybridized carbon, and graphene oxide, the oxidized form of graphene, have attracted considerable attention as potential membrane materials. Both materials can be considered as extremely thin membrane layers consisting of a single layer of atoms. In principle, however, neither graphene nor graphene oxide layers are permeable to liquids or gases, including helium, the smallest gas molecule [89]. A permeable separation membrane is created by producing tiny openings in these layers, e.g., by means of etching processes. Alternatively, graphene or graphene oxide layers can be stacked to produce “few-layer” graphene or graphene oxide, respectively. Their layered structure is comparable to that of graphite. If the layers are stacked in a compact and dense manner, lateral nanochannels are formed that let small molecules such as He , H_2 , or water pass through, but are impermeable to larger molecules [90].

3.2 Fabrication of Porous Membranes

In order to maximize the transport rate, the fabrication of microporous membranes aims to produce layers that are as thin as possible. In practice, mesoporous membrane layers are usually between 1 and $5\text{ }\mu\text{m}$ thick (depending on the membrane material and fabrication process), while microporous membranes are typically less than 200 nm and sometimes less than 50 nm thick. At the same time, defects in the layers, such

as pinholes and cracks, must be avoided because they have a strong impact on the separation properties of the membrane. These technical requirements can be met by employing sol-gel processes and producing the membranes under clean-room conditions.

The majority of mesoporous membrane layers are fabricated using a colloidal sol-gel process. Generally speaking, this involves the hydrolysis of metal alkoxides (e.g., Al-butoxide, Zr-propoxide) by adding water [91, 92]. This results in the formation of a slurry consisting of coagulated nanoparticles, which is converted in a colloidal aqueous system (sol) by adding a so-called peptizing agent (e.g., highly charged ions). Additives such as binders are added to the sol, which is subsequently applied to a macroporous substrate using a thin-film process. A number of different coating technologies are suited for this purpose, e.g., dip coating, spin coating, spray coating, and ink-jet printing, but the latter three are less suitable for coating the inside of tubular geometries. The coating process is followed by a drying step at temperatures of up to 100 °C. The resulting gel film must be heat treated at temperatures of above 400 °C in order to pyrolyze all organic components. For commercialization and series production, fast methods of membrane fabrication are of particular interest. We have therefore implemented rapid thermal processing (RTP), enabling to reduce the time required for heat treatment from 2 d to less than 1 h [77].

Methods for depositing microporous membrane layers can be divided into gas-phase and wet-chemical deposition techniques. Gas-phase methods (e.g., chemical vapor deposition [CVD]) usually produce very dense structures and have so far been applied only in the production of gas separation membranes on a laboratory scale, e.g., in the synthesis of quite dense amorphous SiO₂ layers for H₂ separation [93]. Dip coating is much more attractive for this purpose, both from an economic and a practical perspective. Experience has shown, however, that the colloidal process described above is impracticable for synthesizing layers with pore diameters <2 nm. The most commonly used alternative method is a polymeric sol process. This involves the condensation of partially hydrolyzed metal alkoxide precursor molecules in an alcoholic solution while splitting off water, creating oligomers that form a polymeric network during the coating process [94]. This method is currently used to fabricate microporous layers on the basis of amorphous SiO₂, hybrid SiO₂, and TiO₂, both on a laboratory and an industrial scale. In the area of zeolite membranes, hydrothermal synthesis, which involves the formation of zeolite structures in the presence of a template under hydrothermal conditions, is usually applied. The membrane deposition techniques used include in situ hydrothermal synthesis and colloidal deposition followed by secondary growth. The latter method involves dip coating a colloidal zeolite suspension of seed crystals onto a substrate surface. The seed layer is then grown to form a continuous zeolite film under hydrothermal conditions.

In general, it can be said that the commercial-scale production of membranes with a pore diameter as small as 1 nm is currently feasible. As an example, we would like to point to the work of Petra Puhlfürß et al. at the Fraunhofer Institute for Ceramic Technologies and Systems (IKTS) in Hermsdorf, Germany, who succeeded in producing such membranes on the basis of TiO₂ [84]. These membranes are currently mar-

keted on an industrial scale by the company Inopor GmbH. Other commercial-scale manufacturers of porous ceramic membranes include Atech Innovations GmbH, TAMI GmbH, Pall, GEA, Nanostone, Kerafol, LiqTech, and CTI-ALSYS, all of which sell membranes primarily for microfiltration (MF) and ultrafiltration (UF). As mentioned above, membranes with pore diameters <1 nm for gas separation and pervaporation have also been developed on a laboratory scale. One of the key challenges will be to produce these membranes on an industrial scale with the necessary chemical, thermal, and hydrothermal stability. It should also be mentioned here that preliminary commercial-scale pervaporation/vapor separation applications have already been implemented, e.g., with zeolite membranes [95].



Wilhelm A. Meulenbergh is head of the membranes department at the Institute for Energy and Climate Research 1 at Forschungszentrum Jülich, Germany. He graduated in Metallurgy and Materials Technology as well as Mineralogy at the RWTH Aachen, Germany, where he also obtained his Ph.D. in 1999. Since then, he has been working in Jülich in various areas of materials development and component production. From 2001 to 2003, he was assistant to the Executive Board at Forschungszentrum Jülich and since 2016, he has been a professor at the University of Twente in the field of ion conductors.



Falk Schulze-Küppers is a scientist at the Institute for Energy and Climate Research – IEK-1: Materials Synthesis and Production, Forschungszentrum Jülich. He studied Mechanical Engineering at the RWTH Aachen and received his diploma in 2008. As a doctoral student at IEK-1, he developed thin, supported high-performance membranes. He received his Ph.D. in this field from the Ruhr University Bochum in 2011. Since 2011, he has been the main head of process development and scaling of membrane production at IEK-1.



Wendelin Deibert is a scientist in the team for hydrogen-permeable membranes at the Institute for Energy and Climate Research – IEK-1: Werkstoffsynthese und Herstellungsverfahren, Forschungszentrum Jülich. After graduating with a M.Sc. in Materials Science from RWTH Aachen University in 2012, he joined the team and received his Ph.D. in 2015. He works mainly on the production of ceramic membrane components.



Tim Van Gestel received his Ph.D. in Chemistry from the Catholic University of Leuven, Belgium, in 2003. During his thesis, he did research at Vito in Mol, Belgium, in the field of ceramic porous membranes. Subsequently, he specialized in this field at the University of Twente, Netherlands, for more than two years. At the end of 2005, he started developing ceramic membranes at IEK-1.

His field of research is the pro-

duction of ceramic thin films for separation applications, but also for other energy-related applications such as solid state batteries and fuel cells.



Stefan Baumann is team leader for oxygen-permeable membranes at the Institute for Energy and Climate Research – IEK-1: Werkstoffsynthese und Herstellungsverfahren, Forschungszentrum Jülich. After studying metallurgy and materials engineering at the RWTH Aachen in 1998, he moved to the Institute for Ceramic Components in Mechanical Engineering at the RWTH Aachen, where he dealt

with various topics in technical ceramics and received his Ph.D. in 2007. Since 2006, he has been working at IEK-1 on the material synthesis and processing of gas separation membranes.

References

- [1] W. Deibert, M. E. Ivanova, S. Baumann, O. Guillon, W. A. Meulenbergh, Ion-conducting ceramic membrane reactors for high-temperature applications, *J. Membr. Sci.* **2017**, *543*, 79–97.
- [2] J. Sunarso et al., Mixed ionic-electronic conducting (MIEC) ceramic-based membranes for oxygen separation, *Membr. Sci.* **2008**, *320*, 13–41.
- [3] F. Schulze-Küppers et al., Structural and functional properties of $\text{SrTi}_{1-x}\text{Fe}_x\text{O}_{3-\delta}$ ($0 \leq x \leq 1$) for the use as oxygen transport membrane, *Sep. Purif. Technol.* **2015**, *147*, 414–421.
- [4] Y. Liu, S. Baumann, F. Schulze-Küppers, D. N. Mueller, O. Guillon, Co and Fe co-doping influence on functional properties of SrTiO_3 for use as oxygen transport membranes, *J. Eur. Ceram. Soc.* **2018**, *38*, 5058–5066.
- [5] M. Ramasamy et al., Influence of Microstructure and Surface Activation of Dual-Phase Membrane $\text{Ce}_{0.8}\text{Gd}_{0.2}\text{O}_2\text{-FeCo}_2\text{O}_4$ on Oxygen Permeation, *J. Am. Ceram. Soc.* **2016**, *99*, 349–355.
- [6] J. Seeger et al., Synthesis and characterization of nonsubstituted and substituted proton-conducting $\text{La}_{6-x}\text{WO}_{12-y}$, *Inorg. Chem.* **2013**, *52*, 10375–10386.
- [7] A. Magrasó, R. Haugsrud, Effects of the La/W ratio and doping on the structure, defect structure, stability and functional properties of proton-conducting lanthanum tungstate $\text{La}_{28-x}\text{W}_{4+x}\text{O}_{54+\delta}$. A review, *J. Mater. Chem. A* **2014**, *2*, 12630–12641.
- [8] M. E. Ivanova et al., Influence of $\text{La}_6\text{W}_2\text{O}_{15}$ Phase on the Properties and Integrity of $\text{La}_{6-x}\text{WO}_{12-\delta}$ -Based Membranes, *Chem. Mater. Res.* **2012**, *2*, 56–81.
- [9] S. Escolástico, C. Solís, T. Scherb, G. Schumacher, J. M. Serra, Hydrogen separation in $\text{La}_{5.5}\text{WO}_{11.25-\delta}$ membranes, *J. Membr. Sci.* **2013**, *444*, 276–284.
- [10] D. van Holt et al., Ceramic materials for H_2 transport membranes applicable for gas separation under coal-gasification-related conditions, *J. Eur. Ceram. Soc.* **2014**, *34*, 2381–2389.
- [11] E. Vøllestad, C. K. Vigen, A. Magrasó, R. Haugsrud, Hydrogen permeation characteristics of $\text{La}_{27}\text{Mo}_{1.5}\text{W}_{3.5}\text{O}_{55.5}$, *J. Membr. Sci.* **2014**, *461*, 81–88.
- [12] S. Escolastico, J. Seeger, S. Roitsch, M. Ivanova, W. A. Meulenbergh, J. M. Serra, Enhanced H_2 separation through mixed proton-electron conducting membranes based on $\text{La}_{5.5}\text{W}_{0.8}\text{Mo}_{0.2}\text{O}_{11.25-\delta}$, *ChemSusChem* **2013**, *6*, 1523–1532.
- [13] A. Fantin et al., Relation between composition and vacant oxygen sites in the mixed ionic electronic conductors $\text{La}_{5.4}\text{W}_{1-y}\text{M}_y\text{O}_{12-\delta}$ ($\text{M} = \text{Mo}, \text{Re}; 0 \leq y \leq 0.2$) and their mother compound $\text{La}_{6-x}\text{WO}_{12-\delta}$ ($0.4 \leq x \leq 0.8$), *Solid State Ionics* **2017**, *306*, 104–111.
- [14] R. Haugsrud, T. Norby, Proton conduction in rare-earth ortho-niobates and ortho-tantalates, *Nat. Mater.* **2006**, *5*, 193–196.
- [15] T. Shimura, M. Komori, H. Iwahara, Ionic conduction in pyrochlore-type oxides containing rare earth elements at high temperature, *Solid State Ionics* **1996**, *86–88*, 685–689.
- [16] T. Norby, Solid-state protonic conductors: principles, properties, progress and prospects, *Solid State Ionics* **1999**, *125*, 1–11.

- [17] H. Iwahara, T. Esaka, H. Uchida, N. Maeda, Proton Conduction in Sintered Oxides and its Application to Steam Electrolysis for Hydrogen Production, *Solid State Ionics* **1981**, 3–4, 359–363.
- [18] K. D. Kreuer, Proton-Conducting oxides, *Annu. Rev. Mater. Res.* **2003**, 33, 333–359.
- [19] K.-D. Kreuer, Aspects of the formation and mobility of protonic charge carriers and the stability of perovskite-type oxides, *Solid State Ionics* **1999**, 125, 285–302.
- [20] H. G. Bohn, T. Schober, Electrical Conductivity of the High-Temperature Proton Conductor $\text{BaZr}_{0.9}\text{Y}_{0.1}\text{O}_{3-\delta}$, *J. Am. Ceram. Soc.* **2000**, 83, 768–772.
- [21] H. Iwahara, H. Uchida, K. Ono, K. Ogaki, Proton Conduction in Sintered Oxides Based on BaCeO_3 , *J. Electrochem. Soc.* **1988**, 135 (2), 529–533.
- [22] S. Ricote, N. Bonanos, A. Manerbino, W. G. Coors, Conductivity study of dense $\text{BaCe}_x\text{Zr}_{0.9-x}\text{Y}_{0.1}\text{O}_{3-\delta}$ prepared by solid state reactive sintering at 1500 degrees C, *Int. J. Hydrogen Energy* **2012**, 37, 7954–7961.
- [23] E. Rebollo et al., Exceptional hydrogen permeation of all-ceramic composite robust membranes based on $\text{BaCe}_{0.65}\text{Zr}_{0.20}\text{Y}_{0.15}\text{O}_{3-\delta}$ and Y- or Gd-doped ceria, *Energy Environ. Sci.* **2015**, 8, 3675–3686.
- [24] S. Baumann, W. A. Meulenber, H. P. Buchkremer, Manufacturing strategies for asymmetric ceramic membranes for efficient separation of oxygen from air, *J. Eur. Ceram. Soc.* **2013**, 33, 1251–1261.
- [25] T. Norby, R. Haugsrud, Dense Ceramic Membranes for Hydrogen Separation, in *Nonporous Inorganic Membranes* (Eds: A. F. Sammells, M. V. Mundscha), Wiley-VCH Verlag, Weinheim **2006**.
- [26] K.-D. Kreuer, Proton Conductivity: Materials and Applications, *Chem. Mater.* **1996**, 8, 610–641.
- [27] M. L. Fontaine, T. Norby, Y. Larring, T. Grande, R. Bredeken, Oxygen and Hydrogen Separation Membranes Based on Dense Ceramic Conductors, *Membr. Sci. Technol.* **2008**, 13, 401–458.
- [28] S. Baumann, J. M. Serra, M. P. Lobera, S. Escolástico, F. Schulze-Küppers, W. A. Meulenber, Ultrahigh oxygen permeation flux through supported $\text{Ba}_{0.5}\text{Sr}_{0.5}\text{Co}_{0.8}\text{Fe}_{0.2}\text{O}_{3-\delta}$ membranes, *J. Membr. Sci.* **2011**, 377, 198–205.
- [29] F. Schulze-Küppers, S. Baumann, F. Tietz, H. J. M. Bouwmeester, W. A. Meulenber, Towards the fabrication of $\text{La}_{0.98-x}\text{Sr}_x\text{Co}_{0.2}\text{Fe}_{0.8}\text{O}_{3-\delta}$ perovskite-type oxygen transport membranes, *J. Eur. Ceram. Soc.* **2014**, 34, 3741–3748.
- [30] P. Niehoff et al., Oxygen transport through supported $\text{Ba}_{0.5}\text{Sr}_{0.5}\text{Co}_{0.8}\text{Fe}_{0.2}\text{O}_{3-\delta}$ membranes, *Sep. Purif. Technol.* **2014**, 121, 60–67.
- [31] J. M. Serra, J. Garcia-Fayos, S. Baumann, F. Schulze-Küppers, W. A. Meulenber, Oxygen permeation through tape-cast asymmetric all- $\text{La}_{0.6}\text{Sr}_{0.4}\text{Co}_{0.2}\text{Fe}_{0.8}\text{O}_{3-\delta}$ membranes, *J. Membr. Sci.* **2013**, 447, 297–305.
- [32] W. Deibert, M. E. Ivanova, W. A. Meulenber, R. Vaßen, O. Guillon, Preparation and sintering behaviour of $\text{La}_{5.4}\text{WO}_{12-\delta}$ asymmetric membranes with optimised microstructure for hydrogen separation, *J. Membr. Sci.* **2015**, 492, 439–451.
- [33] W. Deibert, F. Schulze-Küppers, E. Forster, M. E. Ivanova, M. Müller, W. A. Meulenber, Stability and sintering of MgO as a substrate material for Lanthanum Tungstate membranes, *J. Eur. Ceram. Soc.* **2017**, 37, 671–677.
- [34] S. Baumann, P. Niehoff, F. Schulze-Küppers, M. Ramasamy, W. A. Meulenber, O. Guillon, The Role of Solid-Gas Electrochemical Interfaces for Mixed Ionic Electronic Conducting Oxygen Transport Membranes, *ECS Trans.* **2015**, 66 (2), 21–33.
- [35] F. Schulze-Küppers, S. Baumann, W. A. Meulenber, D. Stöver, H. P. Buchkremer, Manufacturing and performance of advanced supported $\text{Ba}_{0.5}\text{Sr}_{0.5}\text{Co}_{0.8}\text{Fe}_{0.2}\text{O}_{3-\delta}$ (BSCF) oxygen transport membranes, *J. Membr. Sci.* **2013**, 433, 121–125.
- [36] F. Schulze-Küppers et al., Comparison of freeze-dried and tape-cast support microstructure on high-flux oxygen transport membrane performance, *J. Membr. Sci.* **2018**, 564, 218–226.
- [37] M. Lipinska-Chwalek, F. Schulze-Küppers, J. Malzbender, Mechanical properties of pure and doped cerium oxide, *J. Eur. Ceram. Soc.* **2015**, 35, 1539–1547.
- [38] R. O. Silva, J. Malzbender, F. Schulze-Küppers, S. Baumann, M. Krüger, O. Guillon, Creep behaviour of dense and porous $\text{SrTi}_{0.75}\text{Fe}_{0.25}\text{O}_{3-\delta}$ for oxygen transport membranes and substrates, *J. Eur. Ceram. Soc.* **2018**, 38, 5067–5073.
- [39] Y. Zou, F. Schulze-Küppers, M. Balaguer, J. Malzbender, M. Krüger, Creep behavior of porous $\text{La}_{0.6}\text{Sr}_{0.4}\text{Co}_{0.2}\text{Fe}_{0.8}\text{O}_{3-\delta}$ substrate material for oxygen separation application, *J. Eur. Ceram. Soc.* **2018**, 38, 1702–1710.
- [40] M. Lipinska-Chwalek, G. Pecanac, J. Malzbender, Creep behaviour of membrane and substrate materials for oxygen separation units, *J. Eur. Ceram. Soc.* **2013**, 33, 1841–1848.
- [41] M. C. Steil, J. Fouletier, P.-M. Geffroy, Surface exchange polarization vs. gas concentration polarization in permeation through mixed ionic-electronic membranes, *J. Membr. Sci.* **2017**, 541, 457–464.
- [42] M. Reichmann, P.-M. Geffroy, N. Richet, T. Chartier, Impact of microstructure on oxygen semi-permeation performance of perovskite membranes: Understanding of oxygen transport mechanisms, *J. Power Sources* **2016**, 324, 774–779.
- [43] B. A. v. Hassel, Oxygen transfer across composite oxygen transport membranes, *Solid State Ionics* **2004**, 174, 253–260.
- [44] J. F. Vente, W. G. Haije, R. Ijpelaar, F. T. Rusting, On the full-scale module design of an air separation unit using mixed ionic electronic conducting membranes, *J. Membr. Sci.* **2006**, 278, 66–71.
- [45] R. E. Mislser, E. R. Twina, *Tape Casting Theory and Practice*, Wiley, New York **2000**.
- [46] W. Schafbauer et al., Tape Casting as a Multipurpose Shaping Technology for Different Applications in Energy Issues, *Mater. Sci. Forum* **2012**, 706–709, 1035–1040.
- [47] R. Kiebach et al., Joining of ceramic $\text{Ba}_{0.5}\text{Sr}_{0.5}\text{Co}_{0.8}\text{Fe}_{0.2}\text{O}_3$ membranes for oxygen production to high temperature alloys, *J. Membr. Sci.* **2016**, 506, 11–21.
- [48] P. I. Dahl et al., Fabrication, sealing and high pressure testing of tubular $\text{La}_2\text{NiO}_{4+\delta}$ membranes for air separation, *Energy Procedia* **2012**, 23, 187–196.
- [49] L. Blum et al., Solid Oxide Fuel Cell Development at Forschungszentrum Juelich, *Fuel Cells* **2007**, 7 (3), 204–210.

- [50] L. Blum et al., SOFC Stack and System Development at Forschungszentrum Jülich, *J. Electrochem. Soc.* **2015**, *162*, F1199–F1205.
- [51] C. Buysse et al., Development, performance and stability of sulfur-free, macrovoid-free BSCF capillaries for high temperature oxygen separation from air, *J. Membr. Sci.* **2011**, *372*, 239–248.
- [52] M. Schulz, U. Pippardt, L. Kiesel, K. Ritter, R. Kriegel, Oxygen permeation of various archetypes of oxygen membranes based on BSCF, *AIChE J.* **2012**, *58*, 3195–202.
- [53] O. Ravkina, T. Klande, A. Feldhoff, Investigation of Zr-doped BSCF perovskite membrane for oxygen separation in the intermediate temperature range, *J. Solid State Chem.* **2013**, *201*, 101–106.
- [54] S. M. Fang, C.-Y. Yoo, H. J. M. Bouwmeester, Performance and stability of niobium-substituted $\text{Ba}_{0.5}\text{Sr}_{0.5}\text{Co}_{0.8}\text{Fe}_{0.2}\text{O}_{3-\delta}$ membranes, *Solid State Ionics* **2011**, *195*, 1–6.
- [55] X. Meng, N. Yang, B. Meng, X. Tan, Z.-F. Ma, S. Liu, Zirconium stabilized $\text{Ba}_{0.5}\text{Sr}_{0.5}(\text{Co}_{0.8x}\text{Zr}_x)\text{Fe}_{0.2}\text{O}_3$ – a perovskite hollow fibre membranes for oxygen separation, *Ceram. Int.* **2011**, *37*, 2701–2709.
- [56] J. Zhu, S. Guo, Z. Zhang, X. Jiang, Z. Liu, W. Jin, CO_2 -tolerant mixed-conducting multi-channel hollow fiber membrane for efficient oxygen separation, *J. Membr. Sci.* **2015**, *485*, 79–86.
- [57] P. Haworth, S. Smart, J. Glasscock, J. C. D. d. Costa, High performance yttrium-doped BSCF hollow fibre membranes, *Purif. Technol.* **2012**, *94*, 16–22.
- [58] H. Gasparyan, J. B. Claridge, M. J. Rosseinsky, Oxygen permeation and stability of Mo-substituted BSCF membranes, *J. Mater. Chem. A* **2015**, *3*, 18265–18272.
- [59] M.-L. Fontaine et al., Fabrication and H_2 flux measurement of asymmetric $\text{La}_{27}\text{W}_{3.5}\text{Mo}_{1.5}\text{O}_{55.5-\delta}$ – $\text{La}_{0.87}\text{Sr}_{0.13}\text{CrO}_{3-\delta}$ membranes, *J. Eur. Ceram. Soc.* **2018**, *38*, 1695–1701.
- [60] S. Escolastico, C. Solis, R. Haugrud, A. Magraso, J. M. Serra, On the ionic character of H_2 separation through mixed conducting $\text{Nd}_{5.5}\text{W}_{0.5}\text{Mo}_{0.5}\text{O}_{11.25-\delta}$ membran, *Int. J. Hydrogen Energy* **2017**, *42*, 11392–11399.
- [61] Y. Cao, N. Duan, L. Jian, A. Evans, R. Haugrud, J. Ihlefeld, Effect of Nb Doping on Hydration and Conductivity of $\text{La}_{27}\text{W}_5\text{O}_{55.5-\delta}$, *J. Am. Ceram. Soc.* **2016**, *99* (10), 3309–3316.
- [62] Y. Chen, S. Cheng, L. Chen, Y. Wei, P. J. Ashman, H. Wang, Niobium and molybdenum co-doped $\text{La}_{5.5}\text{WO}_{11.25-\delta}$ membrane with improved hydrogen permeability, *J. Membr. Sci.* **2016**, *510*, 155–163.
- [63] J. M. Polfus et al., Enhanced O_2 Flux of $\text{CaTi}_{0.85}\text{Fe}_{0.15}\text{O}_{3-\delta}$ Based Membranes by Mn Doping, *J. Am. Ceram. Soc.* **2016**, *99*, 1071–1078.
- [64] C. Gaudillere, J. Garcia-Fayos, M. Balaguer, J. M. Serra, Enhanced oxygen separation through robust freeze-cast bilayered dual-phase membranes, *ChemSusChem* **2014**, *7*, 2554–2561.
- [65] H. Huang, S. Cheng, J. Gao, C. Chen, J. Yi, Phase-inversion tape-casting preparation and significant performance enhancement of $\text{Ce}_{0.9}\text{Gd}_{0.1}\text{O}_{1.95-\delta}$ – $\text{La}_{0.6}\text{Sr}_{0.4}\text{Co}_{0.2}\text{Fe}_{0.8}\text{O}_{3-\delta}$ dual-phase asymmetric membrane for oxygen separation, *Mater. Lett.* **2014**, *137*, 245–248.
- [66] X. Shao, D. Dong, G. Parkinson, C.-Z. Li, A microchanneled ceramic membrane for highly efficient oxygen separation, *Mater. Chem. A* **2013**, *1*, 9641–9644.
- [67] S. Cheng et al., High-Performance Microchanneled Asymmetric $\text{Gd}_{0.1}\text{Ce}_{0.9}\text{O}_{1.95-\delta}$ – $\text{La}_{0.6}\text{Sr}_{0.4}\text{FeO}_{3-\delta}$ -Based Membranes for Oxygen Separation, *ACS Appl. Mater. Interfaces* **2016**, *8*, 4548–4560.
- [68] Z.-X. Low, Y. T. Chua, B. M. Ray, D. Mattia, I. S. Metcalfe, D. A. Patterson, Perspective on 3D printing of separation membranes and comparison to related unconventional fabrication techniques, *J. Membr. Sci.* **2017**, *523*, 596–613.
- [69] Project HETMOC: Highly Efficient Tubular Membranes for Oxy-Combustion, **2014**. https://cordis.europa.eu/project/rcn/100474_de.html
- [70] Project GREEN-CC: Graded Membranes for Energy Efficient New Generation Carbon Capture Process, **2017**. https://cordis.europa.eu/project/rcn/109591_de.html
- [71] Project GREEN-CC: New membrane technology for efficient carbon capture, **2017**. https://cordis.europa.eu/result/rcn/231865_en.html
- [72] F. Schulze-Küppers et al., Design and fabrication of large-sized planar oxygen transport membrane components for direct integration in oxy-combustion processes, *Sep. Purif. Technol.* **2019**, *220*, 89–101.
- [73] Project ELECTRA: High temperature electrolyser with novel proton ceramic tubular modules of superior efficiency, robustness, and lifetime economy, **2017**. https://cordis.europa.eu/project/rcn/185722_en.html
- [74] L. L. Anderson et al., Advances in ion transport membrane technology for oxygen and syngas production, *Solid State Ionics* **2016**, *288*, 331–337.
- [75] S. Duscher, Keramische Membranen für die Filtration von Flüssigkeiten: Eine Bestandsaufnahme. Teil 1: Membrantypen und ihre Betriebsweise, *Fe&S, Filtr. Sep.* **2013**, *27* (4), 200–205.
- [76] S. Duscher, Keramische Membranen für die Filtration von Flüssigkeiten: Eine Bestandsaufnahme. Teil 2: Stofftransport und Ausblicke, *Fe&S, Filtr. Sep.* **2013**, *27* (5), 292–295.
- [77] T. Van Gestel, F. Hauler, M. Bram, W. A. Meulenbergh, H. P. Buchkremer, Synthesis and characterization of hydrogen-selective sol-gel SiO_2 membranes supported on ceramic and stainless steel supports, *Sep. Purif. Technol.* **2014**, *121*, 9–20.
- [78] T. Van Gestel, D. Sebold, Hydrothermally stable mesoporous ZrO_2 membranes prepared by a facile nanoparticle deposition process, *Sep. Purif. Technol.* **2019**, *221*, 399–407.
- [79] R. S. A. de Lange, J. H. A. Hekkink, K. Keizer, A. J. Burggraaf, Permeation and separation studies on microporous sol-gel modified ceramic membranes, *Microporous Mater.* **1995**, *4*, 169–186.
- [80] S. Battersby, T. Tasaki, S. Smart, B. Ladewig, S. Liu, M. C. Duke, V. Rudolph, J. C. Diniz da Costa, Performance of cobalt silica membranes in gas mixture separation, *J. Membr. Sci.* **2009**, *329*, 91–98.
- [81] G. Xomeritakis, C. Y. Tsai, Y. B. Jiang, C. J. Brinker, Tubular ceramic-supported sol-gel silica-based membranes for flue gas carbon dioxide capture and sequestration, *J. Membr. Sci.* **2009**, *341*, 30–36.
- [82] H. L. Casticum, A. Sah, R. Kreiter, D. H. A. Blank, J. F. Vente, J. E. ten Elshof, Hybrid ceramic nanosieves: stabilizing

- nanopores with organic links, *Chem. Commun.* **2008**, 2008 (9), 1103–1105.
- [83] R. Vacassy, C. Guizard, V. Thoraval, L. Cot, Synthesis and characterisation of microporous zirconia powders. Application in nanofiltration characteristics, *J. Membr. Sci.* **1997**, 132, 109–118.
- [84] P. Puhlfürß, I. Voigt, R. Weber, M. Morbé, Microporous TiO₂ membranes with a cut-off <500 Da, *J. Membr. Sci.* **2000**, 174, 123–133.
- [85] M. B. Rao, S. Sircar, Nanoporous carbon membrane for gas separation, *Gas Sep. Purif.* **1993**, 7, 279–284.
- [86] B. Elyassi, M. Sahimi, T. T. Tsotsis, Silicon carbide membranes for gas separation applications, *J. Membr. Sci.* **2007**, 288, 290–297.
- [87] T. Bein, Synthesis and Applications of Molecular Sieve Layers and Membranes, *Chem. Mater.* **1996**, 8, 1636–1653.
- [88] M. Kanezashi, J. O'Brien, Y. S. Lin, Template-free synthesis of MFI-type zeolite membranes: Permeation characteristics and thermal stability improvement of membrane structure, *J. Membr. Sci.* **2006**, 286, 213–222.
- [89] R. R. Nair, H. A. Wu, P. N. Jayaram, I. V. Grigorieva, A. K. Geim, Unimpeded permeation of water through helium leak-tight graphene-based membranes, *Science* **2012**, 335, 442–444.
- [90] T. Van Gestel, J. Barthel, New types of graphene-based membranes with molecular sieve properties for He, H₂ and H₂O, *J. Membr. Sci.* **2018**, 554, 378–384.
- [91] A. F. M. Leenaars, K. Keizer, A. J. Burggraaf, The preparation and characterization of alumina membranes with ultra-fine pores, Part 1. Microstructural investigations on non-supported membranes, *J. Mater. Sci.* **1984**, 19, 1077–1088.
- [92] A. F. M. Leenaars, A. J. Burggraaf, The preparation and characterisation of alumina membranes with ultrafine pores. Part 2. The formation of supported membranes, *J. Colloid Interface Sci.* **1985**, 105, 27–40.
- [93] S. T. Oyama, D. Lee, P. Hacırlıoglu, R. F. Saraf, Theory of hydrogen permeability in nonporous silica membranes, *J. Membr. Sci.* **2004**, 244, 45–53.
- [94] C. J. Brinker, G. W. Scherer, *Sol-Gel Science: The Physics and Chemistry of Sol-Gel Processing*, Academic Press, New York **1990**.
- [95] H. Richter, Zeolithmembranen – Stand der Entwicklung und Anwendung, *Chem. Ing. Tech.* **2012**, 84 (8), 1427–1428.